*Chapter 3*

# CONSTRAINING OPTIMIZED EXCHANGE

## *Marcel Swart,[a,b,c] Miquel Solà[b] and F. Matthias Bickelhaupt[a]*

[a] Department of Theoretical Chemistry and Amsterdam
Center for Multiscale Modeling, Vrije Universiteit Amsterdam,
De Boelelaan 1083, 1081 HV Amsterdam, The Netherlands
[b] Institut de Química Computacional and Departament de Química,
Universitat de Girona, Campus Montilivi, 17071 Girona, Catalunya (Spain)
[c] Institució Catalana de Recerca i Estudis Avançats (ICREA),
08010 Barcelona, Catalunya (Spain)

## Abstract

Several recent studies (*J. Phys. Chem. A* 2004, *108*, 5479; *J. Comput. Chem.* 2007, *28*, 2431) have shown impressive results when replacing the non-empirical PBE density functional by the empirical OPBE or OLYP functionals, i.e. replacing the PBE exchange functional by Handy and Cohen's OPTX functional. To investigate the origin of the improvements, we have placed constraints from the non-empirical PBE exchange functional on the empirical OPTX exchange functional, and tested the performance of the resulting constrained functionals for several characteristic chemical properties. The performance of the new functionals is tested for a number of standard benchmark tests, such as the atomization energies of the G2 set, accuracy of geometries for small molecules, atomic exchange energies, and proton affinities of anionic and neutral molecules. Furthermore, the new functionals are tested against a benchmark set of nucleophilic substitution $S_N2$ reactions, for which we have recently compared DFT with high-level coupled cluster CCSD(T) data (*J. Comput. Chem.* 2007, *28*, 1551). Our study makes clear that the performance depends critically on the number of constraints, and on the reference data to which the constrained functionals are optimized. For each of these properties studied, there is at least one functional that performs very well. Although a new promising functional ($ML_{ff}OLYP$) emerged from the set of constrained functionals that approaches coupled-cluster accuracy for geometries and performs very well for the energy profile of $S_N2$ reactions, there is no one of the newly constructed functionals that performs equally well for all properties.

**Keywords:** Density Functional Theory – Exchange functional – Geometry – Reactivity – Properties.

# Introduction

Over the past twenty years, Density Functional Theory (DFT)[1-3] has become the method of choice for many investigations of chemical problems by quantum-chemistry methods. Within DFT, only the exchange-correlation energy $E_{XC} = E_X + E_C$ as a functional of the electron density $\rho(r)$ must be approximated, i.e. as $E_{XC}[\rho(r)]$. In fact, Hohenberg and Kohn[4] proved that if a suitable functional is chosen, this would give exact results. Unfortunately, they did not give the formulation for this suitable (i.e. exact) functional, for which various approximations have been proposed since then (see the "Formulation of DFT functionals" section). The first and most simple approximation (Local Density Approximation, LDA)[5-7] was derived from the uniform electron gas, and is determined completely by the density $\rho(r)$. Although this approximation works very well for physics, its performance for chemistry was less satisfactory. Therefore, also the density gradient ($\nabla\rho$) was taken into account (Generalized Gradient Approximation, GGA),[8] which indeed showed marked improvements over LDA. Later studies included not only the density gradient, but also its Laplacian ($\nabla^2\rho$) and/or the kinetic energy density (Meta-GGA, MGGA).[9] These three classes (LDA, GGA, MGGA) comprise the first three rungs on Jacob's ladder of increasing accuracy (and complexity).[10] The early GGA functionals were still not as accurate as hoped for, which also led to the inclusion of a portion of Hartree-Fock exchange in the exchange part of the functional (hybrid functionals).[11] In the fourth rung of the ladder (Hyper-GGAs, HGGA), not simply a portion but the full 100% of HF exchange will be taken into account.[12]
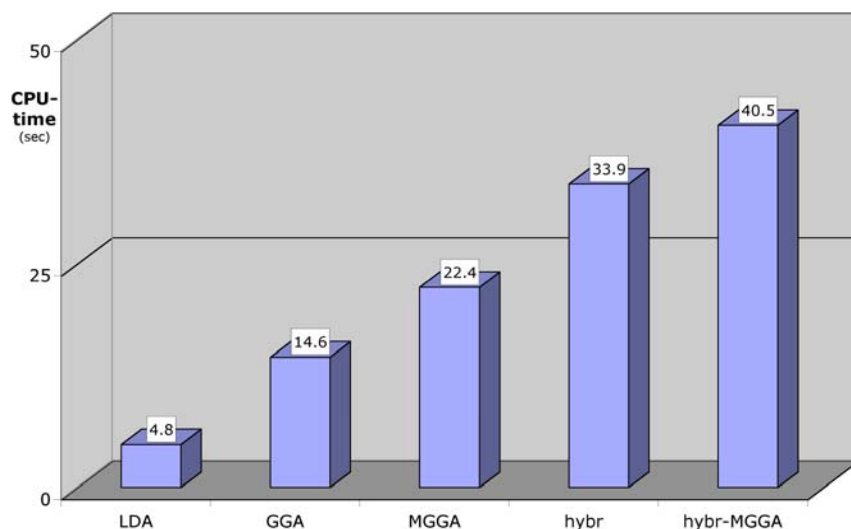


Figure 1. Computational demand (CPU-time, s) of LDA, GGA, MGGA, hybrid and hybrid-MGGA functionals for one SCF cycle for the HOF molecule with the cc-pVQZ basis.

The increase of accuracy (and complexity) comes with a price, as the computational cost increases significantly along the rungs of the ladder (see figure 1). However, because the energy depends in principle only on the density $\rho(r)$ (and its derivatives), which in turn is a

function of only 3 coordinates (x, y, z), DFT is still a much more efficient method than wavefunction ($\Psi$) based methods that explicitly depend on $3N_{elec}$, that is, the 3 coordinates of each of the $N_{elec}$ electrons in the system. Moreover, because of additional enhancements to make the programs more efficient (linear scaling techniques),[13,14] the computational cost of DFT nowadays scales linearly with system size (N), in contrast to for instance the "gold standard" CCSD(T) that scales as $N^7$.[15] Therefore, nowadays it is already possible to treat a complete protein structure of 4728 atoms completely with DFT methods,[16] while probably the largest system studied with CCSD(T) is octane (26 atoms), which was possible only in parallel on ca. 1500 nodes.[17] However, despite the huge computational cost, the CCSD(T) method is highly popular because it is generally applicable and a very accurate method, often even more accurate than experiment.[18-20] As a result, the method is often used in benchmark studies[21-24] to give the reference data with which to compare results from e.g. DFT functionals.

One of the more promising and consistent lines of research within the formulation of DFT functionals is provided by Perdew and co-workers,[6,7,9,12,25-31] who e.g. introduced the first GGA functional. Over the past decades, they have constructed non-empirical functionals on the first three rungs: PW92 (LDA),[7] PBE (GGA),[28,32] TPSS (MGGA),[30] and semi-non-empirical hybrid functionals PBE0[33] (also known as PBE1PBE) and TPSSh[31] that contain 25% and 10% of HF exchange respectively. These functionals were constructed based (amongst others) on constraints that should be satisfied by the exchange-correlation hole,[28] which is one of the reasons why these functionals in general perform very well. However, for each of these functionals there are properties for which it does not perform very well. For instance, the PBE functional is not very accurate for the atomization energies of a set of molecules (the G2 set, see below), for which it shows a deviation of 16 kcal·mol$^{-1}$. Although this is only a fraction of the deviation for LDA (83 kcal·mol$^{-1}$),[23] it is ca. four times that of other functionals such as the highly empirical B3LYP (a hybrid functional).[34] Very soon after its publication, the PBE functional was therefore revised[35] with the atomization energies in mind. In this revPBE functional, one of the PBE constraints (see below) was lifted, which indeed improved results for the G2-set atomization energies. However, for the accuracy of geometries of a set of small molecules,[36] PBE performed significantly better, while for other properties the difference between revPBE and PBE is either insignificant or in favor of PBE. Several other modifications of the PBE functional have been proposed (RPBE,[37] mPBE,[38] xPBE[39]), which however do not show a general improvement and suffer from being highly empirical.

It seemed therefore that improvement over PBE could only be obtained by going to higher rungs on the ladder. This changed however in 2001, when Handy and Cohen[40] introduced the optimized exchange (OPTX) functional, which was fitted to minimize the difference with Hartree-Fock exchange energies for atoms (H-Ar). This difference (3.6 kcal·mol$^{-1}$) was indeed substantially lower than that of other popular exchange functionals like Becke88[41] (7.4 kcal·mol$^{-1}$) or PBEx[32] exchange (40.5 kcal·mol$^{-1}$; see below). When combined with the Lee-Yang-Parr (LYP)[42] correlation functional, the resulting OLYP functional was indeed shown to be a major improvement over other GGA functionals,[43] and for organic chemistry reactions it performed better than the B3LYP functional.[44] Similar good results were obtained by combining OPTX with the PBEc correlation functional (to give OPBE).[21,23,45]

The OPBE functional was tested successfully for the spin ground-state of a series of iron complexes,[45] for which early GGA functionals failed completely. The latter functionals (including PBE) showed a tendency to overstabilize low-spin states, and as a result predicted a low-spin (doublet) ground-state for an iron(III) compound ($Fe(N(CH_2$-o-$C_6H_4S)_3)$(1-Me-imidazole)) that was experimentally shown to be high-spin (sextet). For the vertical spin-state splittings (see figure 2 for its definition), a number of DFT functionals correctly predicted the spin ground-state, which include OPBE,[23] Becke00,[46] B3LYP,[34] TPSSh[30,47] and VS98.[48] However, a more stringent check[49,50] on the performance, by looking at the relaxed spin-state splittings (see figure 2 for its definition) for these iron complexes, revealed that only one reliable functional remained: OPBE.
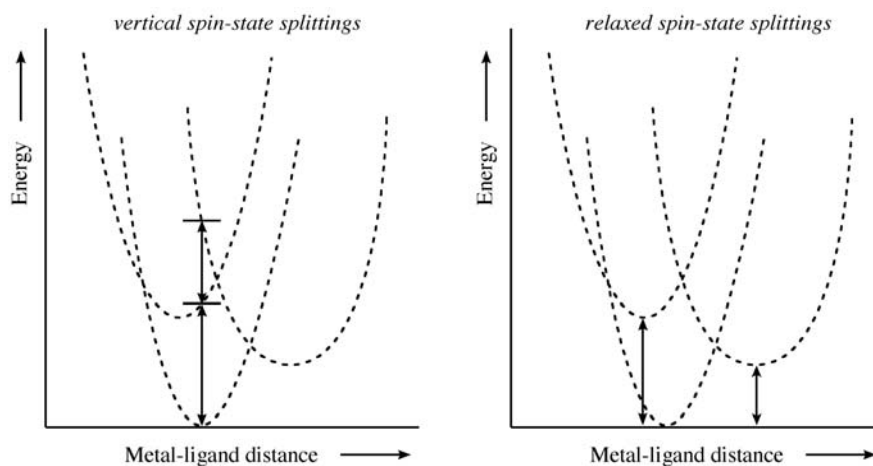


Figure 2. Vertical (left) versus relaxed (right) spin-state splittings.

In a recent study[50] by one of us, the OPBE functional has been used for a series of iron complexes, including a benchmark set ($Fe(II)(H_2O)_6^{2+}$, $Fe(II)(NH_3)_6^{2+}$, $Fe(II)(bpy)_3^{2+}$) for which high-level *ab initio* (CASPT2) data by Pierloot and co-workers[51] are available for comparison. Pierloot and co-workers also used their data to compare with Hartree-Fock (HF) and some DFT functionals, such as LDA, BP86[25,41] (GGA), PBE0[33] (hybrid) and B3LYP[34] (hybrid). These functionals all showed large deviations from the reference data,[51] of respectively 57 (LDA), 15 (BP86), 11 (B3LYP) and 9 (PBE0) kcal·mol$^{-1}$.[50] Moreover, the hybrid functionals B3LYP and PBE0 inadvertently predicted a high-spin (quintet) ground-state for the bipyridyl compound, which should have been low-spin (singlet). This failure of hybrid functionals can be traced directly[52] to the inclusion of a portion of HF exchange; Hartree-Fock itself predicts a high-spin ground-state for all three molecules, with a large deviation (57 kcal·mol$^{-1}$) from the reference CASPT2 data.

The OPBE functional gives excellent agreement[50] with the CASPT2 data for the benchmark set, from which it differs by only 1-2 kcal·mol$^{-1}$. Note that this is an order of magnitude smaller than those of the other DFT functionals, and falls well within the estimated accuracy (1000 cm$^{-1}$ ≈ 3 kcal·mol$^{-1}$) of the CASPT2 data.[51] In the same paper,[50] a number of other difficult iron compounds have been studied that include a spin-crossover compound for which B3LYP and B3LYP* (a reparameterized form[53] of B3LYP that contains only 15% HF exchange instead of the 20% in B3LYP) were shown to fail.[54] For

all these compounds does OPBE give excellent behavior, i.e. it predicts the spin ground-state that is experimentally observed and gives metal-ligand distances that are in good agreement with experimental structures. Of particular interest[50] are two iron compounds based on pyridylmethylamine (pma) ligands, for which the mono-pma compound has a high-spin ground-state, while the di-pma compound has a low-spin ground-state. These two compounds are structurally very similar with a distorted octahedral arrangement of ligands around the iron, in which the only difference is the replacement of a chloride ligand (in mono-pma) by a pyridine ligand (in di-pma). Despite these small changes, the OPBE functional is able to correctly predict the spin ground-state, in contrast to other DFT functionals. The standard pure functionals, which overstabilize low-spin states, fail for the mono-pma compound for which they do not predict the high spin-state. Hybrid functionals, which overstabilize high spin-states due to inclusion of HF exchange, fail for the di-pma compound for which they do not predict the low spin-state. Especially noteworthy was the failure of the Minnesota M06 functionals, which were reported[55] to be the most reliable for organometallic compounds, but nevertheless failed dramatically for the spin ground-states of iron complexes.

The reliability of the OPBE functional for providing spin ground-states has been shown also by studies from other groups,[52,56-68] which also looked at other metals than iron. Furthermore, some of us have investigated[69] its performance for the spin ground-states of a number of ligands, for which experimental data are available with several first-row transition-metals in a number of oxidation states (Mn(II), Mn(III), Mn(IV), Cr(II), Co(II), Co(III), Ni(II), Ni(III), Fe(II), Fe(III)). In all these cases did OPBE correctly predict the spin ground-state.

Recently, we have investigated the influence of the basis set on the spin-state splittings,[70] which was found to be substantial. It was shown that both vertical and relaxed spin-state splittings converge rapidly with basis set size when using Slater-Type Orbitals (STOs), while the convergence is much slower for Gaussian-Type Orbitals (GTOs). The smaller GTO basis sets have in particular problems with high-spin states that are typically placed at too low energy, especially when looking at relaxed spin-state splittings. However, when using very large and demanding GTO basis sets (like NR-cc-pVTZ), the GTO series converges to the same results as obtained with the STO series. This does not occur when using basis sets that include Effective Core Potentials (ECPBs) that give results that are fundamentally different from the STO/GTO data.[70]

The good performance of the OPBE functional for the spin-states of iron complexes concurs with a recent benchmark study on the energy landscapes of bimolecular nucleophilic substitution ($S_N2$) reactions by us.[21] In that study, we investigated the performance of DFT functionals for the energy profile of $S_N2$ reactions for which reference CCSD(T) data were available in the literature. It was shown that functionals based on OPTX exchange (OPBE, OLYP) significantly improve upon early GGA functionals such as BLYP or PBE, i.e. the underestimation of reaction barriers by the latter is dramatically reduced (roughly by a factor of two). Moreover, we also investigated the geometries of the different stationary points (reactants, products, reactant complexes, product complexes, transition states), and compared the resulting structures with the CCSD(T) data. Significant improvements over standard GGA results were obtained by using the OLYP and OPBE functionals, i.e. distances from OLYP/OPBE were twice as accurate while angles were five to ten times as accurate. The overall performance for the geometry, as measured by the $P_G$ value, is therefore ten to twenty times smaller for the more accurate OPBE ($P_G$ value 0.04) and OLYP ($P_G$ value 0.03)

functionals than for standard DFT functionals like BP86 ($P_G$ value 0.34), LDA ($P_G$ value 0.34), PBE ($P_G$ value 0.61) or BLYP ($P_G$ value 0.72). In fact, both OLYP and OPBE performed substantially better for the geometries than either OLAP3[71,72] (MGGA, $P_G$ value 0.07) or mPBE0KCIS (hybrid, $P_G$ value 0.06), which were respectively the best performing MGGA and hybrid functional for the energetics of the $S_N2$ reactions.[21]

In another validation study by some of us,[24] the competing elimination and substitution pathways (*anti*-E2, *syn*-E2, $S_N2$) were determined for $X^-$ + $CH_3CH_2X$ (X= F, Cl) at the CCSD(T)/aug-cc-pVxZ//OLYP/TZ2P level (x=Q for F, T+d for Cl). The same geometries were used to determine the corresponding energies for a range of *ab initio* methods and DFT functionals. The reference CCSD(T) data showed the *anti*-E2 pathway to be most favorable for the fluoride reaction, while for chloride the substitution pathway is most favorable. Most DFT functionals correctly predicted the chloride pathway (apart from M06-2X), but very few GGA and MGGA functionals could correctly predict the *anti*-E2 pathway being most favorable for the fluoride reaction. The exceptions were mainly those (M)GGA functionals based on OPTX exchange (OPBE, OLYP, OLAP3). [24] The best performing GGA functional for both the overall and central barrier was again OPBE, however with a substantial mean absolute deviation (MAD) from the CCSD(T) data of 4.4 and 4.3 kcal·mol$^{-1}$, respectively. Similar to what was observed in the benchmark study on the energy landscapes of $S_N2$ reactions, these deviations show a dramatic reduction compared to early GGAs such as PBE, which showed MAD values of 11.8 and 7.5 kcal·mol$^{-1}$, respectively for the overall and central barrier. As the elimination transition structures involve weak interactions of the nucleophile/leaving group with the substrate (for which OPBE does not work that well, see below), part of the elevated MAD value of OPBE and OLYP might be attributed to the less satisfactory description of these by OPBE and OLYP. It should also be noted that the best performing DFT functional for the $S_N2$ energetics (mPBE0KCIS), now performs significantly less with MAD values close to those of OPBE.

For NMR chemical shifts, OPBE also seems to give good results,[58,59] and was in fact claimed to be the best DFT functional around,[59] often even surpassing the MP2 method, although this has recently been questioned by Truhlar and co-workers.[73] Truhlar claimed that the study by Xu and co-workers[59] was biased by leaving out ozone and PN (for which OPBE supposedly does not perform as well as for $^{13}C$ or $^1H$ NMR), but this does not explain why OPBE gives a much larger deviation for $^{13}C$ chemical shifts (5.8 ppm) in Truhlar's study than in the Wu study (2.3 ppm). Fact is that a different GTO basis set was used in these two studies, which might explain the observed differences. After all, NMR is a nuclear property for which a good description of the region around the nucleus is mandatory, and since GTOs do not have a cusp at the nucleus, they might not be particularly well suited for studying NMR parameters unless very large and demanding basis sets are used (see above for the enormous influence of the basis set type and size on spin-state splittings).

Despite these successes of OPBE for spin-state splittings,[45] $S_N2$ energy landscapes,[21] accuracy of geometries,[23] vibrational frequencies,[23] NMR chemical shifts,[59] there are also examples where it fails dramatically. The most important failings are observed for weak interactions, i.e. π-π stacking[74] and hydrogen-bonding interactions,[75] while it also does not work as well as anticipated for the proton affinities of anionic[76] and neutral[77] bases (see below). These weak interactions are especially important for biochemical systems, in particular for DNA and RNA where inter-strand hydrogen-bonding interactions and intra-strand π-π stacking interactions provide strong binding.[74]

The π-π stacking interaction remains a problematic and difficult interaction for DFT to handle,[74] which is often ascribed to the problems of DFT to describe dispersion interactions. Although it is true that empirical $C/R^6$ corrections[78] sometimes reduce the failings of DFT functionals, there is no causal relation between dispersion and stacking. The best example are posed by the XLYP and X3LYP functionals,[79] which were shown to perform very well for the dispersion interactions of noble-gas dimers ($He_2$, $Ne_2$). Therefore, these "best functionals available at that time" were predicted to perform equally well for π-π stacking interactions of DNA bases;[79] however, they failed badly[80] (also for spin-state splittings[49,50] and $S_N2$ reaction barriers[21]). Recently, some of us investigated how good or bad the DFT functionals are for π-π stacking interactions,[74] and found that there are indeed some functionals (LDA, KT1,[81] KT2,[81] BHandH[82]) that give a very good description for it. For π-π stacking OPBE and OLYP are not particularly good.[74] They even show repulsive interactions, unlike e.g. PBE that still shows attraction (although too weak).

Hydrogen-bonding interactions are in general well described by many DFT functionals, as was recently shown by some of us[75] for the H-bonding interactions in the DNA base pairs A:T and G:C. Among the functionals that perform well are PW91 and BP86, while OPBE and B3LYP underestimate H-bonding interactions. For instance for OPBE, the hydrogen-bond distances were overestimated by 0.05-0.14 Å and the corresponding energy underestimated by 9-12 kcal·mol$^{-1}$. We therefore concluded[74,75,83] that at present there is no DFT functional available that is simultaneously accurate for both weak (intermolecular) and strong (intramolecular) interactions, reaction barriers and spin-state splittings (to name just a few in a wide range of characteristic properties). In order to be able to study e.g. the structure and reactivity of DNA, we designed a multi-level QM/QM approach (QUILD: QUantum-regions Interconnected by Local Descriptions)[83] in which each type of interaction can be studied by that particular methodology that is appropriate for it.

Because of the emerging pattern where PBE works well for some properties, but not for others, and the impressive improvements shown by OPBE, we were interested in finding out what is the origin of the differences observed between PBE and OPBE. In other words, why does OPBE work so much better for reaction barriers and spin-state splittings, and not at all for weak interactions ? Since both functionals contain the same PBEc correlation functional, and differ only in the exchange part, it is obvious that it is determined by exchange. However, exactly which part of it ? In the design of the PBEx exchange functional,[32] Perdew and co-workers used four constraints (see below) that completely determines its formulation. The OPTX functional[40] satisfies only one of these constraints, so it is very likely that releasing the other three leads to the major improvements seen by OPBE. However, are all three important or just one or perhaps none at all ? Here, we investigate this puzzling question in two ways: (i) either by imposing the constraints on the OPTX formula; or (ii) by releasing them for the PBEx formula.

## Formulation of DFT Functionals

Density functional theory methods[1-3] such as the local density approximation (LDA) and the generalized gradient approximation (GGA) describe the exchange-correlation energy in terms of the density $\rho$ and density gradient $\nabla\rho$:

$$E_{XC}^{LDA}\left[\rho_\alpha,\rho_\beta\right]= \int d^3r \;\; \varepsilon_{XC}^{unif}\left(\rho_\alpha,\rho_\beta\right)$$
$$E_{XC}^{GGA}\left[\rho_\alpha,\rho_\beta\right]= \int d^3r \;\; f\left(\rho_\alpha,\rho_\beta,\nabla\rho_\alpha,\nabla\rho_\beta\right)$$

(1)

The expression for the exchange energy of LDA is derived from the uniform electron gas and is formulated as $C_X\cdot\rho^{4/3}$, with $C_X$ a constant and $\rho$ the (spin-polarized) density. Because there is no exchange taking place between electrons of opposite spin, for spin-polarized systems the exchange energy is simply the sum of the separate energies in terms of $\alpha$ and $\beta$ density; see the spin-scaling relationship below (constraint **iv**).[32] The expression for the LDA correlation energy is a bit more involved,[5,7] and since we are focusing here on the exchange energy only, it will not be given explicitly. The formula of the GGA exchange energy can be expressed as function of the LDA exchange energy, by using an enhancement factor *F(s)* that is expressed in terms of the reduced density gradient $s = |\nabla\rho| \,/\, 2\rho k_F$, $k_F{}^3=[3\pi^2\cdot\rho]$:[8]

$$E_X^{GGA} = \int d^3r \;\; \varepsilon_X^{unif}\left(\rho\right)\cdot F\left(s\right)$$

(2)

In 1996, Perdew, Burke and Ernzerhof (PBE)[32] introduced a simplification of the earlier Perdew-Wang (PW91) functional,[26] both of which contain only physical constants as parameters. Moreover, they posed[32] a set of four constraints on the exchange part of the (PBEx) functional that completely determines its expression:

i) to recover the correct uniform gas limit, the exchange functional should have an enhancement factor *F(s)* that equals 1 (i.e. LDA) when the reduced density gradient *s* is zero

ii) at low values of *s*, i.e. for small density variations around the uniform density, the functional should have a limiting behavior that goes as $\sim 1+\mu s^2$ to cancel the correlation-GGA contribution and thus recover the LDA linear response

iii) the Lieb-Oxford bound,[10] which should be met, will be satisfied if the enhancement factor grows gradually with *s* to a maximum value of 1.804

iv) the exact exchange energy obeys the spin-scaling relationship:

$$E_X\left[\rho_\alpha,\rho_\beta\right]= \left(E_X\left[2\rho_\alpha\right]+ E_X\left[2\rho_\beta\right]\right)/2$$

(3)

A simple expression that satisfies these four constraints is given by their chosen form for the enhancement factor[32]

$$F^{PBE}\left(s\right)=\left[A + Cs^2 \frac{1}{1+\frac{C}{B}s^2}\right]= A + B\frac{1}{1+\frac{B}{C}s^{-2}}$$

(4)

with A=1.0, B=0.804 and C≈0.219515. Note that the limiting behavior for both s→0 (in square brackets) and s→∞ are given in Eq. 4.

The OPTX functional by Handy and Cohen[40] satisfies only constraint **iv**, and has the following expression for the enhancement factor:

$$F^{OPTX}(s) = A + B\frac{C^2 s^4}{\left(1 + Cs^2\right)^2} = A + Bu^2 \quad ; \quad u = \frac{Cs^2}{1 + Cs^2} \tag{5}$$

with A=1.05151, B=1.538582 and C=0.364624. One of the main differences is therefore that whereas the PBEx exchange functional has $s^2$ as leading term, for OPTX it is $s^4$. One of us therefore argued in a previous validation study for the spin-states of iron complexes,[45] that this difference in leading terms could be responsible for the improvements observed for the OPBE functional. Here we will see if that assessment still holds, or if it is determined more by the constraints that are imposed on the exchange functional.

We also include a third expression for the exchange enhancement factor, which was derived from a Bayesian Error Estimate (BEEx)[84] and which is some kind of mixture between the PBE and OPTX expressions:

$$F^{BEE}(s) = A + \frac{Bs^2}{\left(1 + s\right)^2} + \frac{Cs^4}{\left(1 + s\right)^4} \tag{6}$$

with A=1.0008, B=0.1926, C=1.8962. The BEEx expression is combined with PBEc correlation.

The expression for the correlation energy in the PBE functional (PBEc) is given by the following formula:

$$E_C^{GGA} = \int d^3 r \, \rho \left[ \varepsilon_C^{unif}(\rho, \zeta) + H(\rho, \zeta, t) \right] \tag{7}$$

with $\zeta$ the relative spin polarization $(\rho_{up} - \rho_{down})/\rho_{total}$, and $t$ another dimensionless (reduced) density gradient, which depends on the spin-scaling factor $\phi$ and the Thomas-Fermi screening wave number $k_s$:

$$t = \frac{|\nabla \rho|}{2\phi(\zeta) \cdot k_s \cdot \rho} \quad ; \quad \phi(\zeta) = \frac{(1+\zeta)^{2/3} + (1-\zeta)^{2/3}}{2} \quad ; \quad k_s = \sqrt{\frac{4k_f}{\pi}} \quad ; \quad k_f = \left(3\pi^2 \cdot \rho\right)^{1/3} \tag{8}$$

The function $H$ in eq. 7 is determined by three conditions,[32] for the slowly varying limit (t→0), for the rapidly varying limit (t→∞) and uniform scaling, which are satisfied by the following ansatz:

$$H^{PBE}(\rho, \zeta, t) = \gamma \phi^3 \cdot \ln \left[ 1 + \frac{\beta}{\gamma} t^2 \cdot \frac{1 + At^2}{1 + At^2 + A^2 t^4} \right] \quad ; \quad A = \frac{\beta}{\gamma} \frac{1}{\exp\left(\frac{\varepsilon_C^{unif}}{\gamma \phi^3}\right) - 1} \tag{9}$$

In the slowly varying limit t→0 (the term in square brackets), this is therefore slightly different than the corresponding exchange expression (see term in square brackets in eq. 4). For that reason, we implemented also the simplified expression for PBE correlation (sPBEc), with the only difference with eq. 9 in the term in square brackets:

$$H^{sPBE}(\rho,\zeta,t) = \gamma\phi^3 \cdot \ln\left[1 + \frac{\beta}{\gamma}t^2 \cdot \frac{1}{1+At^2}\right] \qquad (10)$$

Combined with the original PBEx exchange expression this makes the sPBE functional.

## Benchmark Systems

We used a range of characteristic properties in order to investigate the performance of the newly obtained functionals, ranging from atomic (H-Ar) exchange energies; standard benchmark sets like G2 atomization energies, accuracy of geometries and proton affinities; weak interactions, i.e. π-π stacking interactions in DNA bases and hydrogen-bonding in small molecules; energy landscapes of $S_N2$ reactions; to geometric parameters of stationary points in the $S_N2$ reactions. Below, we report for each set where the reference data are coming from, and specific details about the reference set.

### Atomic Exchange Energies for H-Ar

The atomic exchange energies from Hartree-Fock are many times used as reference values to validate or construct DFT functionals. Indeed, the OPTX functional[40] was constructed based on fitting the parameters and functional form to reproduce as best as possible the atomic exchange energies for H to Ar. In our tests on the atomic exchange energies, we compare our computed energies with the Hartree-Fock values that were taken directly from the OPTX paper.

### Atomization Energies for the G2-1 and G2/97 Sets

The atomization energy of a molecule consists of its bonding energy with respect to the sum of the energies of the isolated (spin-polarized) atoms. A number of reference sets are available (such as the G2-1[85] or G2/97[86]) that are often used to compare DFT functionals. Here, we use the geometries and reference energies ($\Delta E_{el}$) as given by Curtiss and co-workers,[1] for either the G2-1 set (55 molecules) or the G2/97 set (148 molecules).

### Accuracy of Geometries for a Set of Small Molecules

Helgaker and co-workers[18,20] investigated the basis set dependence for a set of small molecules, using a number of *ab initio* methods. They observed excellent results (0.1-0.2 pm) using CCSD(T)/cc-pVxZ (x=T,Q,5) and showed an experimental error for one of the molecules.[20] Previously,[23,36] one of us used this set of molecules to test the basis set dependence and influence of the DFT functionals on the accuracy of the geometries. Early GGA functionals were shown to give deviations of ca. 1 pm,[36] while functionals containing OPTX showed somewhat smaller deviations (0.6-0.9 pm).[23] The set of molecules consists

of the following molecules: HF, $H_2O$, $NH_3$, $CH_4$, $N_2$, $CH_2$, CO, HCN, $CO_2$, HNC, $C_2H_2$, $CH_2O$, HNO, $N_2H_2$, $O_3$, $C_2H_4$, $F_2$, HOF, $H_2O_2$.
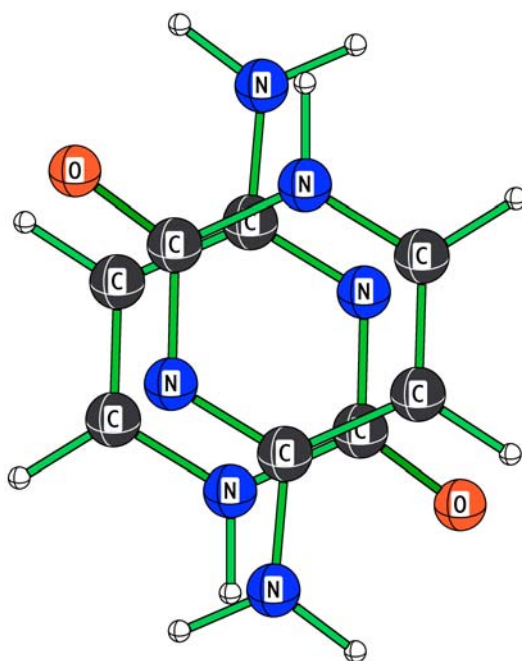


Figure 3. Geometry of 180° twisted cytosine dimer used for $\pi$-$\pi$ stacking benchmark.

## Proton Affinities of Anionic and Neutral Bases

The proton affinity of an anionic or neutral base B is related to the enthalpy change at 298K for the following reaction: BH $\rightarrow$ B + H ($\Delta H$ = –PA). In a series of papers,[76,77,87] some of us investigated the PA values for a range of anionic and neutral bases ($2^{nd}$ to $6^{th}$ period hydrides for group 14-18), and studied how these are affected by methyl substitution and solvation. These studies also included validation of the DFT functionals[76,77] by comparing with CCSD(T) data. Early GGA functionals like BP86 and PBE showed deviations from the CCSD(T) data of ca. 1.5 kcal·mol$^{-1}$, while the values for OLYP and OPBE are significantly larger (see below). The same reference geometries and energies as previously were used, and the same basis set strategy. I.e. we used the TZ2P basis for optimizing the geometry, and the QZ4P basis in the subsequent single-point energy calculation. The set of anionic bases consists of $CH_3^-$, $C_2H_3^-$, $NH_2^-$, $C_6H_5^-$, $H^-$, $HCO^-$, $OH^-$, $CH_3O^-$, $CH_3CH_2O^-$, $C_2H^-$, $(CH_3)_2CHO^-$, $(CH_3)_3CO^-$, $F^-$, $SH^-$, $CN^-$, $Cl^-$, $Br^-$,[76] while the set of neutral bases consists of $NH_3$, $CH_2CO$, $H_2O$, CO, $CO_2$, $N_2$.[77]

---

[1] http://chemistry.anl.gov/compmat/comptherm.htm

## The π-π Stacking in DNA Bases

Recently,[74] we compared the performance of DFT functionals for π-π stacking interactions in DNA bases and analogs. Here, we take one prototypical example (stacked cytosine, see figure 3) and examine the deviation of the DFT functionals from a reference CCSD(T) value of -9.93 kcal·mol$^{-1}$, which was taken from ref. [88]. The vertical distance is 3.3 Å and the upper cytosine is rotated by 180° compared to the lower (around the center of mass of the upper cytosine).[88]

## Hydrogen-Bonding Interactions

Sponer, Hobza and co-workers[89] proposed a set of weakly bound dimer systems that can be used to validate other methods. The geometries of the hydrogen-bonded dimer systems were mainly obtained at MP2, but for four dimers (of ammonia, water, formamide, formic acid; see figure 4) they had been obtained at the CCSD(T) level. These four were therefore used here to compare the DFT functionals with. In particular, the distances indicated in figure 4 were used for comparison with the CCSD(T)/cc-pVxZ (x=T for formic acid and formamide dimer, x=Q for ammonia and water dimer) distances.



ammonia dimer                                        water dimer

formamide dimer                                      formic acid dimer
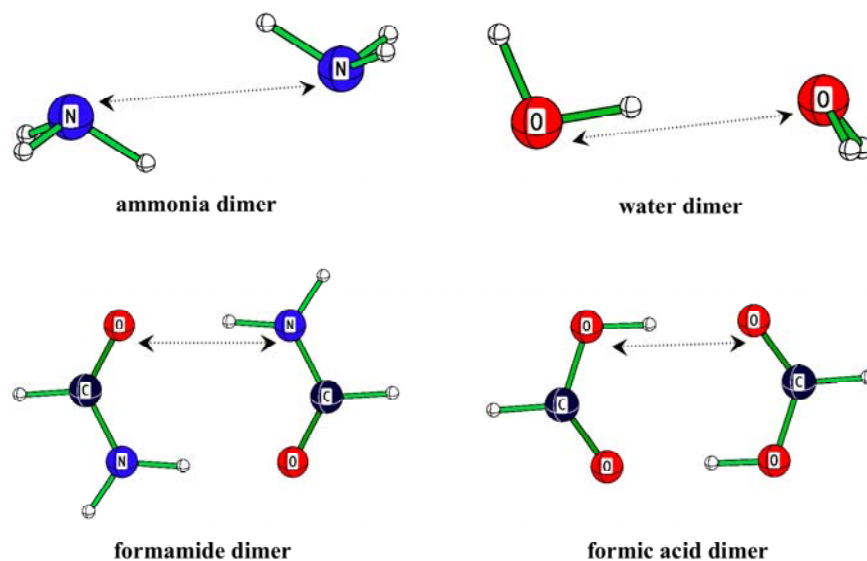
Figure 4. Geometries of the hydrogen-bonded dimers (indicated with arrows are the distances that are used for comparison with the CCSD(T) data).

## Energy Landscapes of S$_N$2 Reactions

In a recent paper,[21] we reported a study on the comparison between DFT and CCSD(T) for the energy landscapes of gas-phase S$_N$2 reactions (see figure 5 for a typical energy profile). We showed that there was in general good agreement between DFT and CCSD(T) and that this coherence was better when large basis sets were used in both the CCSD(T) and

DFT. Here, we therefore look only at those reactions for which the reference data were coming from studies where CCSD(T) was used for obtaining both the energy and the geometry, and with large basis sets. In the terminology of that paper, we take only reactions **A2** to **A6** into account (see tables 1 and 2 of Ref. 21).
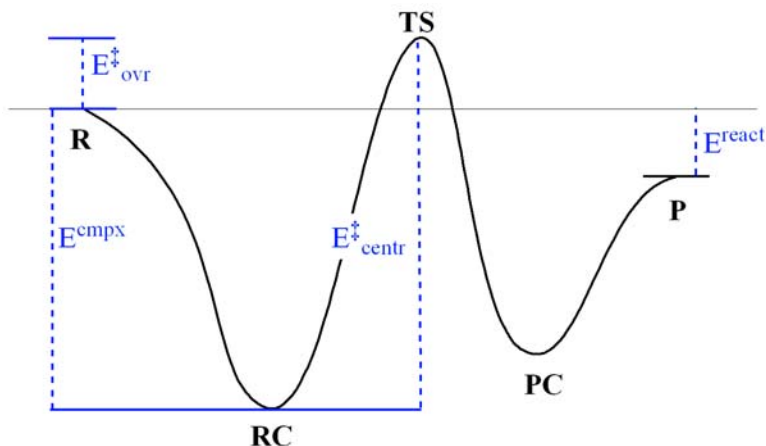


Figure 5. Energy profile for $S_N2$ reactions.

## Structural Characterization of Stationary Points for $S_N2$ Reactions

Similar to the energy landscapes (see above),[21] for the structural characterization of $S_N2$ reactions we only look at those that were obtained using CCSD(T) with a large basis set. Therefore, the set of reactions for which the stationary points were determined by the DFT functionals (and compared to CCSD(T)) consists of the following reactions: $Cl^- + CH_3Br \rightarrow CH_3Cl + Br^-$, $F^- + CH_3Cl \rightarrow CH_3F + Cl^-$, $Cl^- + CH_3Cl \rightarrow CH_3Cl + Cl^-$, $Br^- + CH_3Br \rightarrow CH_3Br + Br^-$, $F^- + CH_3F \rightarrow CH_3F + F^-$.

## Spin-State Splittings of a High-Spin Iron Compound

Previously,[45,50] we have shown that the OPBE functional works exceptionally well for spin-states of iron complexes, and we therefore include one of the typical molecules for which early GGAs were found to fail, which is the compound $Fe(N(CH_2\text{-}o\text{-}C_6H_4S)_3)(1\text{-Me-imidazole})$. Experimentally and with OPBE, it has a high-spin sextet ground-state.

# Computational Details

All DFT calculations were performed with a locally adapted version of the Amsterdam Density Functional (ADF, version 2006.01)[90,91] program developed by Baerends et al. The MOs were expanded in a large uncontracted set of Slater-type orbitals (TZ2P, QZ4P),[92] which are respectively of triple-$\zeta$ quality augmented by two sets of polarization functions, and of quadruple-$\zeta$ quality augmented by four sets of polarization functions.[91] An auxiliary set

of *s*, *p*, *d*, *f*, and *g* STOs was used to fit the molecular density and to represent the Coulomb and exchange potentials accurately in each SCF cycle. All energies and gradients were calculated with the local density approximation (LDA) and generalized gradient approximation (GGA) corrections added self-consistently.

**Table 1. Overview of expression of exchange functionals studied (see text for further details) and Mean Absolute Deviations (kcal·mol$^{-1}$) against atomic exchange energies**

| functional | type[a,b,c] | A | B | C | MAD in $E_x$[d] |
|---|---|---|---|---|---|
| OPTX | optx | 1.05151 | 1.538582 | 0.364624 | 3.73 |
| PBEx | pbe | 1.0 | 0.804 | 0.219515 | 40.48 |
| BEEx | bee | 1.0008 | 0.1926 | 1.8962 | 75.49 |
| **optimized against atomic exchange** | | | | | |
| $A_{ff}$PBEx | pbe | 1.0246 | 4.3704 | 0.1450 | 4.26 |
| $A_{fp}$PBEx | pbe | 1.0116 | 0.7924 | 0.2018 | 6.97 |
| $A_{lf}$PBEx | pbe | 1.0 | 0.7843 | 0.2397 | 8.32 |
| $A_{lp}$PBEx | pbe | 1.0 | 0.804 | 0.2386 | 8.39 |
| $A_{ff}$O | optx | 1.0508 | 1.5303 | 0.3687 | 2.94 |
| $A_{fp}$O | optx | 1.0416 | 0.7624 | 0.7034 | 5.30 |
| $A_{lf}$O | optx | 1.0 | 0.3505 | 2.6018 | 10.77 |
| $A_{lp}$O | optx | 1.0 | 0.804 | 1.1152 | 30.32 |
| **optimized against atomization energies of G2-1 set** | | | | | |
| MP$_{ff}$PBEx | pbe | 1.0807 | 1.7144 | 0.2497 | 689.72 |
| MP$_{fp}$PBEx | pbe | 1.0092 | 0.7948 | 0.4232 | 456.67 |
| MP$_{lf}$PBEx | pbe | 1.0 | 1.0446 | 0.2551 | 75.73 |
| MP$_{lp}$PBEx | pbe | 1.0 | 0.804 | 0.3826 | 315.29 |
| ML$_{ff}$O | optx | 1.0728 | 1.5124 | 0.4214 | 221.28 |
| ML$_{fp}$O | optx | 1.0141 | 0.7899 | 0.9191 | 35.65 |
| ML$_{lf}$O | optx | 1.0 | 1.2783 | 0.4004 | 380.54 |
| ML$_{lp}$O | optx | 1.0 | 0.804 | 0.8354 | 184.75 |
| MP$_{ff}$O | optx | 1.0890 | 1.4234 | 0.5050 | 416.84 |
| MP$_{fp}$O | optx | 1.0266 | 0.7774 | 1.0742 | 151.10 |
| MP$_{lf}$O | optx | 1.0 | 1.1567 | 0.4629 | 348.10 |
| MP$_{lp}$O | optx | 1.0 | 0.804 | 0.8680 | 161.63 |

a) pbe: $F(s) = A + B \cdot Cs^2/(B + Cs^2)$

b) optx: $F(s) = A + B \cdot u^2$ ; $u = (C \cdot s^2)/(1 + C \cdot s^2)$

c) bee: $A + B \cdot s^2/(1+s)^2 + C \cdot s^4/(1+s)^4$

d) mean absolute deviations (kcal·mol$^{-1}$) from Hartree-Fock atomic exchange energies for H-Ar.

The newly developed functionals are labeled (X$_{ab}$) according to the reference data (X) to which they were optimized and the constraints that are imposed on it (*ab*). The reference data can be either A for atomic exchange (Hartree-Fock) energies of H-Ar, or MP cq. ML for experimental molecular atomization energies of the G2-1 set; MP when obtained in combination with PBEc correlation, and ML when obtained in combination with LYPc correlation. The labeling of the constraints (*ab=ff, fp, lf, lp*) refers to the constraint at s=0 (*a=l* for LDA, constraint **i**; *a=f* for free, i.e. no constraint) and at s=∞ (*b=p* for PBE maximum of

constraint **iii**; *b=f* for free, i.e. no constraint). For instance, $A_{fp}$ refers to the functional optimized against atomic exchange energies, with the Perdew maximum (constraint **iii**) imposed on the enhancement factor with the LDA limit at s=0 not imposed (see also table 1 for the expression of the functionals).

## Construction of the New Functionals

Handy and Cohen constructed their OPTX functional[40] by optimizing the atomic exchange energies of H-Ar against those from Hartree-Fock using a large basis, ending up with a deviation of 3.6 kcal·mol$^{-1}$ between the two methods. This is significantly better than the Becke88[41] functional (7.4 kcal·mol$^{-1}$), or PBE[32] (40.5 kcal·mol$^{-1}$). In the first part of this study, we also optimize our functionals against the atomic exchange energies from Hartree-Fock, in four different combinations (see table 1 for the parameters of the exchange functionals thus obtained). The first combination ($A_{ff}O$) imposes no constraint at all, i.e. similar to the OPTX functional. Indeed we do find similar performance for the atomic exchange energies with a mean absolute deviation (MAD) of 2.9 kcal·mol$^{-1}$ (see table 1). The slight improvement over the original OPTX functional (MAD value 3.7 kcal·mol$^{-1}$) probably results from our fit procedure, which might be slightly different from that of Handy and Cohen. If we now impose constraint **iii** (Lieb-Oxford bound)[32] on the enhancement factor, to give the $A_{fp}O$ functional, the MAD value for the HF exchange energies increases to 5.3 kcal·mol$^{-1}$. On the other hand, imposing the constraint for the LDA limit (constraint **i**), the MAD value increases to 10.8 kcal·mol$^{-1}$. By imposing both these constraints, the MAD value goes up to 30.3 kcal·mol$^{-1}$ (see table 1). The smaller deviation of OPTX compared to the PBEx functional is therefore resulting directly from the enhanced flexibility of not imposing constraints on the A and C parameters. At first sight, it might seem that the improved performance is also resulting from the exchange expression of OPTX, if one compares the MAD value of $A_{lp}O$ functional (30.3 kcal·mol$^{-1}$) with that of PBEx (40.5 kcal·mol$^{-1}$). However, this is not a fair comparison since the C parameter is in PBEx fixed by constraint **ii**, while it is freely optimized in $A_{lp}O$. A better comparison is therefore made by looking at the $A_{lp}PBEx$ functional, in which the C parameter was also optimized freely. Its MAD value for the HF exchange energies (8.4 kcal·mol$^{-1}$) is many times smaller than that of the $A_{lp}O$ functional, which indicates in itself that the PBEx expression is "better" for exchange than the OPTX expression. In fact, the value for the C-parameter within $A_{lp}PBEx$ (0.2386) is only 9% larger than the constrained value (~0.2195). By optimizing also either the A or the B parameter, the MAD value for HF exchange energies is reduced further, but only nominally, to 8.3 kcal·mol$^{-1}$ for $A_{lf}PBEx$ and 7.0 kcal·mol$^{-1}$ for $A_{fp}PBEx$ (see table 1). Only by optimizing all three parameters simultaneously does a further reduction to 4.3 kcal·mol$^{-1}$ occur, but with a limit for s→∞ (5.395) that is unrealistically high (the OPTX functional that violates both the local and integrated Lieb-Oxford bounds has a limiting behavior of "only" 2.59). Therefore, the relatively large MAD value of PBEx (40.5 kcal·mol$^{-1}$) for the HF exchange energies of H-Ar is largely reduced by lifting either one of constraints **i**, **ii**, or **iii**. In fact, the $A_{lf}PBEx$ functional, in which the maximum on the enhancement factor is not imposed, results in a value for the B parameter that is actually lower than the one that is set by the Lieb-Oxford bound. In other words, even though it is not constrained to satisfy the Lieb-

Oxford bound, it still does ! The downside is however that it is now no longer a non-empirical functional.

Although many exchange functionals have been obtained by comparing with atomic exchange (as Handy and Cohen did for OPTX),[40] there are also many (empirical) functionals that have been fitted to, for instance, the atomization energies of the G2-1 set.[34,38,85,93,94] Examples of the latter are, for instance, the B3PW91 functional by Becke,[11] who for the first time introduced the concept of hybrid functionals, or HCTH.[93] Therefore, we decided to also construct functionals by optimizing the parameters of the exchange expression for the atomization energies of the G2-1 set. In this second part, we therefore have to include a functional for the correlation energy, which was chosen to be the PBEc for the $MP_{ab}PBE$ and $MP_{ab}OPBE$ functionals, and LYPc for the $ML_{ab}OLYP$ functionals. It is interesting to note that for the completely free functionals ($MP_{ff}PBE$, $ML_{ff}OLYP$, $MP_{ff}OPBE$), the deviation from the LDA limit (A=1.0) is substantially larger than for the atomic functionals of the first part. For instance, the value for the A parameter increases from 1.0508 (for $A_{ff}O$) to 1.0728 ($ML_{ff}O$) or 1.0890 ($MP_{ff}O$) (see table 1), and similarly from 1.0246 for $A_{ff}PBEx$ to 1.0807 for $MP_{ff}PBEx$. Furthermore, the value for the B parameter is for the molecular functionals in this second part found to be substantially larger than the Lieb-Oxford bound (0.804), with values of 1.0446 for $MP_{lf}PBEx$, 1.2783 for $ML_{lf}O$ and 1.1567 for $MP_{lf}O$. Note that in the first part, even though the B parameter was not constrained to the Lieb-Oxford bound, it still did satisfy it. For the molecular functionals, this no longer holds.

For the molecular functionals of this second part, the mean absolute deviation (MAD) for the G2-1 set[85] ranges from 2.5 to 5.5 kcal·mol$^{-1}$ (see table 2). This is a major improvement over the MAD values for the combination of the atomic functionals from the first part with their respective correlation functionals, which showed MAD values from 3.1 to 14.8 kcal·mol$^{-1}$. It is interesting to see that for each of the three types of molecular functionals introduced here ($MP_{ab}PBE$, $ML_{ab}OLYP$ and $MP_{ab}OPBE$) that the completely free form (ab=ff) gives a significant better performance than the other three forms (ab=fp,lf,lp), which give more or less the same MAD values. This is in particular true for the $MP_{ab}PBE$ functionals, where the $MP_{ff}PBE$ functional has a MAD value of 3.1 kcal·mol$^{-1}$, while the other three have MAD values of 4.7-4.9 kcal·mol$^{-1}$, despite the very different values for the A,B,C parameters of the various molecular functionals.

The good performance of the molecular functionals does not coincide with equally good performance for the atomic exchange energies (see table 2). Apart from the $ML_{fp}OLYP$ functional, whose MAD value of 35.7 kcal·mol$^{-1}$ for atomic exchange is similar to that of PBEx, and the $MP_{lf}PBE$ functional, whose value of 75.7 kcal·mol$^{-1}$ is comparable to that of BEE, for the others a significantly larger MAD value is observed with values between 150 and 690 kcal·mol$^{-1}$. So it seems that by fitting to molecular properties, one is losing the accuracy for the atomic properties. We also experimented briefly by optimizing simultaneously the atomic exchange and G2-1 atomization energies (more specifically, by minimizing the product of their respective MAD values), but this basically lead to small variations on the atomic functionals of the first part and will thus not be discussed any further. The smallest deviation is observed for the $ML_{ff}OLYP$ functional.

**Table 2. Mean absolute deviation (MAD) values for standard benchmark studies[a] (kcal·mol⁻¹, pm)**

| functional | atomic exchange | G2-1 | G2/97 | geom. 1st row[c] | PA anionic | PA neutrals | π-π stacking | hydrogen-bonding |
|---|---|---|---|---|---|---|---|---|
| basis set used | QZ4P | QZ4P | QZ4P | TZ2P | QZ4P | QZ4P | TZ2P | TZ2P |
|  | (kcal·mol⁻¹) | (kcal·mol⁻¹) | (kcal·mol⁻¹) | (pm) | (kcal·mol⁻¹) | (kcal·mol⁻¹) | (kcal·mol⁻¹) | (pm) |
| PBE | 40.48 | 7.95 | 16.32 | 0.87 | 1.63 | 1.45 | 7.14 | 2.46 |
| sPBE | 40.48 | 6.80 | 12.94 | 0.92 | 1.62 | 1.49 | 7.19 | 1.90 |
| BEE | 75.49 | 5.32 | 8.03 | 1.00 | 1.73 | **1.17** | 10.65 | 5.64 |
| OPBE | 3.73 | 4.79 | 8.90 | 0.90 | 5.54 | 3.83 | 15.62 | 28.11 |
| OLYP | 3.73 | 3.24 | 4.24 | 0.64 | 2.89 | 1.42 | 14.43 | 23.20 |
| A$_{ff}$PBE | *4.26* | 4.69 | 44.61 | 0.76 | 4.68 | 3.51 | 18.15 | 30.44 |
| A$_{fp}$PBE | *6.97* | 10.16 | 23.45 | 0.68 | 1.51 | 1.36 | 6.82 | 4.44 |
| A$_{1f}$PBE | *8.32* | 7.38 | 14.47 | 0.86 | 1.49 | 1.42 | 6.91 | 1.93 |
| A$_{1p}$PBE | *8.39* | 7.08 | 13.58 | 0.87 | **1.48** | 1.39 | 7.13 | **1.83** |
| A$_{ff}$OLYP | *2.94* | 3.10 | 4.23 | 0.65 | 2.87 | 1.40 | 14.41 | 23.55 |
| A$_{fp}$OLYP | *5.30* | 10.49 | 21.47 | 0.64 | 1.85 | 1.86 | 6.85 | 3.39 |
| A$_{1f}$OLYP | *10.77* | 14.82 | 29.49 | 0.74 | 7.71 | 5.77 | 0.72 | 8.49 |
| A$_{1p}$OLYP | *30.32* | 7.14 | 20.38 | 2.16 | 3.57 | 2.21 | 7.49 | 17.39 |
| A$_{ff}$OPBE | *2.94* | 4.66 | 8.41 | 0.90 | 5.49 | 3.82 | 15.59 | 28.53 |
| A$_{fp}$OPBE | *5.30* | 10.91 | 27.00 | 0.78 | 2.39 | 1.59 | 8.05 | 3.62 |
| A$_{1f}$OPBE | *10.77* | 14.59 | 34.31 | 0.74 | 4.48 | 3.20 | **0.26** | 11.21 |
| A$_{1p}$OPBE | *30.32* | 7.16 | 15.52 | 1.75 | 1.90 | 1.66 | 8.39 | 17.23 |
| MP$_{ff}$PBE | 689.72 | *3.07* | **3.94** | 1.01 | 11.94 | 6.16 | 13.38 | 16.75 |
| MP$_{fp}$PBE | 456.67 | *4.77* | 7.08 | 0.69 | 3.20 | 1.33 | 5.98 | 2.34 |
| MP$_{1f}$PBE | 75.73 | *4.71* | 7.09 | 1.01 | 1.97 | 1.20 | 9.69 | 7.97 |
| MP$_{1p}$PBE | 315.29 | *4.87* | 9.42 | 0.82 | 2.10 | 1.20 | 6.52 | 3.55 |
| ML$_{ff}$OLYP | 221.28 | *2.51* | 4.57 | **0.33** | 5.38 | 2.86 | 14.17 | 27.41 |
| ML$_{fp}$OLYP | 35.65 | *4.42* | 8.21 | 1.57 | 3.18 | 2.10 | 7.46 | 13.16 |
| ML$_{1f}$OLYP | 380.54 | *3.99* | 8.85 | 1.83 | 4.49 | 1.81 | 13.21 | 20.41 |
| ML$_{1p}$OLYP | 184.75 | *4.61* | 9.73 | 1.95 | 4.74 | 5.99 | 9.04 | 14.50 |
| MP$_{ff}$OPBE | 416.84 | *3.47* | 4.71 | 0.61 | 10.96 | 6.48 | 14.34 | 35.41 |
| MP$_{fp}$OPBE | 151.10 | *5.09* | 6.73 | 0.91 | 2.54 | 1.67 | 7.70 | 11.80 |
| MP$_{1f}$OPBE | 348.10 | *5.19* | 7.07 | 1.56 | 2.79 | 1.30 | 13.33 | 21.40 |
| MP$_{1p}$OPBE | 161.63 | *5.47* | 7.50 | 1.61 | 2.13 | 1.50 | 9.04 | 14.50 |

[a] in *italics* are the values which were used to construct the functionals in this chapter, in **bold** the functional that performs best for that particular property.

# Performance of the Functionals for Standard Benchmark Studies

Apart from the atomization energies for the G2-1 set,[85] we subjected the functionals also to other standard benchmark studies, such as the atomization energies for the larger and more diverse G2/97 set,[86] the accuracy of geometries of first-row molecules,[18,20,36] proton affinities of anionic and neutral bases,[76,77] and weak interactions ($\pi$-$\pi$ stacking[74,88] and hydrogen-bonding[89]).

## Atomization Energies

For many functionals considered here, going from the G2-1 set[85] with small molecules to the more diverse G2/97 set[86] with medium-sized molecules results in a doubling of the MAD value. A similar pattern was observed by Perdew and co-workers[47] for the MAD values of several methods for the G2/97 and G3/3 set (that contains even larger molecules), which doubled[47] for e.g. Hartree-Fock (148.3 [G2/97] vs. 336.4 [G3/3] kcal·mol$^{-1}$), LDA (83.7 vs. 197.1 kcal·mol$^{-1}$), PBE (16.9 vs. 32.8 kcal·mol$^{-1}$) or B3LYP (3.1 vs. 8.4 kcal·mol$^{-1}$). Surprisingly,[47] the MAD values decreased for their TPSS (6.0 [G2/97] vs. 5.5 kcal·mol$^{-1}$) and TPSSh (4.2 vs. 3.3 kcal·mol$^{-1}$) functionals.

Here, we see in most cases also a doubling of the MAD value for the G2/97 set compared to that of the G2-1 set. For instance, the values for OPBE are 4.8 and 8.9 kcal·mol$^{-1}$, for $A_{lf}$PBE 7.4 and 14.5 kcal·mol$^{-1}$, and 4.9 and 9.4 kcal·mol$^{-1}$ for $MP_{lp}$PBE, to name but a few. However, there also exceptions, both in the positive and negative sense. The MAD value for OLYP increases only from 3.2 kcal·mol$^{-1}$ for G2-1 to 4.2 for G2/97, and that of $MP_{ff}$OPBE from 3.5 to 4.7 kcal·mol$^{-1}$. On the other hand, for $A_{ff}$PBE it increases from 4.7 kcal·mol$^{-1}$ for G2-1 to 44.6 kcal·mol$^{-1}$ for G2/97. This is probably the result of the limit for large $s$ of this functional (see above). Although the $ML_{ff}$OLYP was the best performing functional for the G2-1 set, it is no longer so for the larger G2/97 set, for which a MAD value of 4.6 kcal·mol$^{-1}$ is observed. For the G2/97 set, the best performance is shown by the $MP_{ff}$PBE functional, which was already second-best for the G2-1 set, with a MAD value of 3.9 kcal·mol$^{-1}$.

## Accuracy of Geometries

Previously,[23,36] one of us investigated the accuracy of geometries of a number of early GGAs, and found the best performance for amongst others PBE (ca. 1.0 pm), while a later study[23] showed the improved performance of OPBE and OLYP (0.8-0.9 pm). Although this is still far from the accuracy obtained by the "gold standard" CCSD(T), which showed deviations of ca. 0.1-0.2 pm, it is still a major improvement over Hartree-Fock that gave deviations of 2.9 pm.[18] In comparison to the previous study,[23] where a TZP basis was used, here we use the larger TZ2P basis set. Both PBE and OLYP significantly increase their accuracy by ca. 0.3 pm, to 0.9 pm (PBE) and 0.6 pm (OLYP), while OPBE gives the same deviation as it had with the TZP basis (0.9 pm). Many of the newly developed atomic functionals provide deviations that are similar to those of OPBE and OLYP, with mean absolute deviations between 0.6 and 0.9 pm (see table 2), and few that give much larger deviations such as $A_{lp}$OLYP (deviation 2.2 pm) or $A_{lp}$OPBE (deviation 1.8 pm).

The situation is reversed for the newly developed molecular functionals, where many show larger deviations (between 1.0 and 2.0 pm), and few show deviations that are comparable to OPBE or OLYP. There is however one exception (ML$_{ff}$OLYP) that has an exceptionally good performance for the geometries of this set of small molecules. Its MAD value of 0.3 pm is by far the lowest for any DFT functional, surpasses that of MP2 and CCSD (0.5 pm),[18,20] and approaches the accuracy of the coupled cluster CCSD(T) method.

For the molecular functionals based on the OPTX expression, there is a clear correlation between the amount of constraints that are imposed and the accuracy obtained. I.e., more constraints imposed results directly in an increase of the deviation. This is not true for the molecular PBE functionals, nor for the atomic functionals. For these latter functionals, the best performance is obtained when one constraint is imposed as in A$_{fp}$PBE, A$_{fp}$OLYP, and A$_{lf}$OPBE.

## Proton Affinities of Anionic and Neutral Bases

Recently,[76,77] some of use investigated the proton affinities of anionic and neutral bases for hydrides of the 2$^{nd}$-6$^{th}$ period, and groups 14-18. These studies also involved the validation of DFT functionals for this property by comparing the DFT proton affinity values to those from CCSD(T), where available. It was shown that DFT works in general very well, and has a mean absolute deviation from CCSD(T) (and experiment) of ca 1.5 kcal·mol$^{-1}$. Surprisingly, the deviations were larger for OPBE and (in lesser amount) OLYP than for PBE. Here we find the same for the newly developed functionals based on the OPTX expression, which show deviations between 1.9 and 11.0 kcal·mol$^{-1}$ for anionic bases, and between 1.3 and 6.5 kcal·mol$^{-1}$ for neutral bases (see table 2).

Surprisingly, in many cases and for both the atomic and molecular functionals, the constrained functionals show better performance than the non-constrained (ab=ff) ones. For instance, MP$_{ff}$OPBE gives deviations of 11.0 (anionic bases) and 6.5 (neutral) kcal·mol$^{-1}$, while MP$_{lp}$OPBE gives values of 2.1 and 1.5 kcal·mol$^{-1}$ respectively. The same happens for the atomic counterparts with values of 5.5/3.8 kcal·mol$^{-1}$ for A$_{ff}$OPBE, and values of 1.9/1.7 kcal·mol$^{-1}$ for A$_{lp}$OPBE. Therefore, there is no direct relationship between atomic exchange (or atomization energies of the G2-1 set) on one hand, and the proton affinities at the other. Or at best, there is an anti-correlation between the two sides.

## Weak Interactions

One of the traditionally weak points of DFT is formed by π-π stacking interactions,[74] while hydrogen-bonding interactions are described reasonably well to very good by many functionals.[75] These trends are well shown by the PBE functional, that gives a deviation of 7.1 kcal·mol$^{-1}$ for the π-π stacking of the 180° twisted cytosine dimer, and for a set of four hydrogen-bonded dimers gives a mean absolute deviation of 2.5 pm (see table 2). Note that PBE still predicts an attractive interaction for the π-π stacking (-2.8 kcal·mol$^{-1}$).

The failure of both OPBE and OLYP for weak interactions is immediately obvious from table 2, i.e. they show deviations of 15.6 (OPBE) and 14.4 (OLYP) kcal·mol$^{-1}$ for π-π stacking. Note that this corresponds to repulsive interactions of +5.7 and +4.5 kcal·mol$^{-1}$

respectively. Also for hydrogen-bonding interactions are they not performing well with mean absolute deviations of 28.1 (OPBE) and 23.2 (OLYP) pm. Both functionals predict H-bond distances that are substantially larger than they should be, i.e. they severely underestimate hydrogen-bonding interactions. In a recent study on hydrogen-bonding interactions in DNA bases,[75] we already showed this failure of OPBE.

The performance of the newly developed functionals for the weak interactions shows no general trend, although all functionals without constraints imposed (ab=ff) perform badly for both $\pi$-$\pi$ stacking and hydrogen-bonding interactions. For $\pi$-$\pi$ stacking, these functionals show MAD values between 13.4 and 18.2 kcal·mol$^{-1}$ (all repulsive), while for hydrogen-bonding the MAD values are between 16.8 and 35.4 pm. The functionals with one or more constraint imposed show somewhat smaller MAD values, and in some cases are the best performing functionals. For instance for $\pi$-$\pi$ stacking, the $A_{lf}$OPBE functional has a MAD value of only 0.3 kcal·mol$^{-1}$, which is however not accompanied by an equally good performance for hydrogen-bonding where it shows a MAD value of 11.2 pm. The best performance for hydrogen-bonding is shown by $A_{lp}$PBE, with a MAD value of 1.8 pm, but in a similar fashion to $A_{lf}$OPBE it does not perform equally well for $\pi$-$\pi$ stacking, for which it has a MAD value of 7.1 kcal·mol$^{-1}$.

**Table 3. Deviations$^{a}$ from CCSD(T) results for $S_N2$ reaction energy profiles (kcal·mol$^{-1}$)**

| functional | $\Delta E^{react}$ | $\Delta E^{cmpx}$ | $\Delta E^{\ddagger,centr}$ | $\Delta E^{\ddagger,ovr}$ | $P_E$ |
|---|---|---|---|---|---|
| PBE | 0.34 | 1.49 | 6.43 | 7.78 | 4.01 |
| sPBE | 0.68 | 1.48 | 6.54 | 7.45 | 4.04 |
| BEE | 0.32 | 1.44 | 5.92 | 5.61 | 3.32 |
| OPBE | 0.31 | 3.54 | 3.37 | 1.26 | 2.12 |
| OLYP | 0.50 | 2.58 | 4.14 | 1.69 | 2.23 |
| $A_{ff}$PBE | 0.23 | 4.09 | 4.95 | 0.92 | 2.55 |
| $A_{fp}$PBE | 0.31 | 1.52 | 6.26 | 7.65 | 3.94 |
| $A_{lf}$PBE | 0.34 | 1.55 | 6.53 | 7.99 | 4.10 |
| $A_{lp}$PBE | 0.34 | 1.49 | 6.49 | 7.85 | 4.04 |
| $A_{ff}$OLYP | 0.51 | 2.57 | 4.14 | 1.69 | 2.23 |
| $A_{fp}$OLYP | 0.50 | 1.67 | 5.04 | 6.32 | 3.38 |
| $A_{lf}$OLYP | 0.37 | 5.64 | 8.75 | 14.40 | 7.29 |
| $A_{lp}$OLYP | 0.55 | 1.83 | 5.61 | 7.07 | 3.76 |
| $A_{ff}$OPBE | 0.32 | 3.54 | 3.37 | 1.26 | 2.12 |
| $A_{fp}$OPBE | 0.31 | 1.56 | 4.27 | 4.47 | 2.65 |
| $A_{lf}$OPBE | 0.19 | 4.56 | 7.98 | 12.54 | 6.32 |
| $A_{lp}$OPBE | 0.37 | 1.61 | 4.84 | 5.22 | 3.01 |
| $MP_{ff}$PBE | 0.22 | 2.48 | 4.54 | 2.06 | 2.33 |
| $MP_{fp}$PBE | 0.32 | 1.97 | 7.28 | 9.26 | 4.71 |
| $MP_{lf}$PBE | 0.36 | 1.34 | 6.19 | 6.37 | 3.56 |
| $MP_{lp}$PBE | 0.34 | 1.80 | 7.15 | 8.91 | 4.55 |
| $ML_{ff}$OLYP | 0.49 | 2.87 | 3.56 | 1.44 | 2.09 |
| $ML_{fp}$OLYP | 0.55 | 1.72 | 5.27 | 6.52 | 3.51 |
| $ML_{lf}$OLYP | 0.59 | 2.01 | 5.07 | 3.89 | 2.89 |

**Table 3. Continued.**

| functional | $\Delta E^{react}$ | $\Delta E^{cmpx}$ | $\Delta E^{\ddagger,centr}$ | $\Delta E^{\ddagger,ovr}$ | $P_E$ |
|---|---|---|---|---|---|
| ML$_{1p}$OLYP | 0.58 | 1.71 | 5.37 | 6.47 | 3.54 |
| MP$_{ff}$OPBE | 0.29 | 3.85 | 2.37 | 1.74 | 2.06 |
| MP$_{fp}$OPBE | 0.32 | 1.57 | 4.53 | 4.97 | 2.85 |
| MP$_{1f}$OPBE | 0.41 | 2.10 | 4.28 | 2.40 | 2.30 |
| MP$_{1p}$OPBE | 0.39 | 1.66 | 4.61 | 4.65 | 2.83 |

[a] results obtained using QZ4P basis set, in **bold** the functional that performs best for that particular property.

# Performance of the Functionals for S$_N$2 Energy Landscapes and Structural Characterization

The performance of the functionals for the energy profile of S$_N$2 reactions is measured in terms of four components of the energy profile.[21] These correspond to (see figure 5): the overall reaction energy ($E^{react}$), the complexation energy ($E^{cmpx}$), the central barrier ($E^{\ddagger}_{centr}$) and the overall barrier ($E^{\ddagger}_{ovr}$). The absolute deviation from the reference CCSD(T) data for each component is obtained for each reaction, and averaged over all reactions (**A2-A6**) to give the MAD value for each component. The average of the MAD values for the four components then gives the performance for the energy profile ($P_E$).

Given in table 3 are the MAD values for each component and the $P_E$ value for all functionals considered in this chapter. As already discussed previously,[21] the early GGA functionals like PBE have in particular problems with reaction barriers, which is dramatically reduced by the functionals with OPTX. For instance, the MAD value for the central barrier is 6.4 kcal·mol$^{-1}$ for PBE, 4.1 kcal·mol$^{-1}$ for OLYP and only 3.4 kcal·mol$^{-1}$ for OPBE. This also influences the overall $P_E$ performance considerably, where the value for PBE (4.0 kcal·mol$^{-1}$) is nearly halved for OLYP (2.2 kcal·mol$^{-1}$) and OPBE (2.1 kcal·mol$^{-1}$).

For the newly developed functionals, the best performance is obtained for those without constraints imposed (see table 3). This is in particular true for $P_E$ and the central barrier, for which MP$_{ff}$OPBE performs best with MAD values of 2.1 and 2.4 kcal·mol$^{-1}$ respectively, and the overall barrier, for which A$_{ff}$PBE performs best with a value of 0.9 kcal·mol$^{-1}$. Imposing constraints raises the MAD values of the barriers substantially, but, interestingly, at the same time lowers the MAD values for the complexation energy. The MAD values for the reaction energy seems to be hardly affected by imposing constraints or not, i.e. the MAD value for all functionals is found within the very narrow range of 0.2-0.7 kcal·mol$^{-1}$. The lowering of the MAD value for the complexation energy upon imposing constraints is somewhat consistent with the trend observed for the hydrogen-bonding interactions (see above), where the largest MAD value was shown by the functionals without constraints. However, imposing constraints is not in all cases favorable for the complexation energy, as is shown by e.g. the A$_{lf}$OLYP and A$_{lf}$OPBE functionals. The MAD value for the complexation energy of A$_{lf}$OLYP is more than twice as large as that of the constraint-free A$_{ff}$OLYP functional, leading to an overall $P_E$ value of 7.3 kcal·mol$^{-1}$. This is the largest $P_E$ value in this chapter, and in fact even larger than LDA, which had a $P_E$ value of 5.6 kcal·mol$^{-1}$ for reactions **A2-A6**.

**Table 4. Deviations[a] from CCSD(T) geometries for stationary points of $S_N2$ reactions (Å, deg)[b]**

| functional | $R_{all}$ | $R_{R,P}$ | $R_{RC,PC}$ | $R_{TS}$ | $\theta_{all}$ | $\theta_{R,C}$ | $\theta_{RC,PC}$ | $\theta_{TS}$ | $P_G$ |
|---|---|---|---|---|---|---|---|---|---|
| PBE | 0.101 | 0.010 | 0.139 | 0.078 | 4.134 | 0.082 | 5.581 | 5.145 | 0.418 |
| sPBE | 0.092 | 0.012 | 0.139 | 0.050 | 3.842 | 0.106 | 5.577 | 3.375 | 0.353 |
| BEE | 0.037 | 0.012 | 0.041 | 0.042 | 0.921 | 0.076 | 0.754 | 2.771 | 0.034 |
| OPBE | 0.069 | 0.010 | 0.115 | 0.017 | 0.607 | 0.338 | 0.621 | 0.958 | 0.042 |
| OLYP | 0.063 | 0.007 | 0.095 | 0.034 | 0.463 | **0.049** | 0.396 | 1.317 | 0.029 |
| $A_{ff}$PBE | 0.050 | 0.006 | 0.076 | 0.028 | 0.712 | 0.139 | 0.548 | 2.143 | 0.036 |
| $A_{fp}$PBE | 0.031 | 0.005 | 0.038 | 0.032 | 0.993 | 0.071 | 0.819 | 2.988 | 0.031 |
| $A_{1f}$PBE | 0.102 | 0.011 | 0.139 | 0.081 | 4.668 | 0.100 | 5.606 | 8.241 | 0.476 |
| $A_{1p}$PBE | 0.092 | 0.011 | 0.139 | 0.050 | 3.933 | 0.102 | 5.603 | 3.836 | 0.362 |
| $A_{ff}$OLYP | 0.059 | 0.007 | 0.088 | 0.034 | 0.470 | 0.062 | 0.400 | 1.328 | 0.028 |
| $A_{fp}$OLYP | 0.030 | 0.008 | 0.033 | 0.036 | 0.604 | 0.061 | 0.531 | 1.673 | 0.018 |
| $A_{1f}$OLYP | 0.126 | 0.018 | 0.175 | 0.094 | 4.672 | 0.444 | 6.498 | 4.622 | 0.589 |
| $A_{1p}$OLYP | 0.151 | 0.036 | 0.187 | 0.145 | 4.525 | 0.598 | 6.211 | 4.514 | 0.683 |
| $A_{ff}$OPBE | 0.064 | 0.010 | 0.107 | 0.017 | 0.563 | 0.308 | 0.555 | 0.975 | 0.036 |
| $A_{fp}$OPBE | **0.022** | 0.009 | **0.029** | 0.016 | 0.548 | 0.285 | 0.502 | 1.107 | **0.012** |
| $A_{1f}$OPBE | 0.113 | 0.007 | 0.166 | 0.074 | 4.253 | 0.198 | 5.768 | 5.037 | 0.481 |
| $A_{1p}$OPBE | 0.058 | 0.024 | 0.063 | 0.066 | 0.719 | 0.209 | 0.667 | 1.663 | 0.042 |
| $MP_{ff}$PBE | 0.045 | 0.010 | 0.064 | 0.030 | 0.506 | 0.087 | 0.457 | 1.304 | 0.023 |
| $MP_{fp}$PBE | 0.113 | 0.018 | 0.147 | 0.101 | 4.547 | 0.498 | 6.254 | 4.645 | 0.514 |
| $MP_{1f}$PBE | 0.113 | 0.015 | 0.151 | 0.094 | 4.669 | 0.218 | 5.649 | 7.918 | 0.528 |
| $MP_{1p}$PBE | 0.111 | 0.017 | 0.145 | 0.100 | 5.045 | 0.451 | 6.140 | 8.104 | 0.560 |
| $ML_{ff}$OLYP | 0.063 | **0.004** | 0.097 | 0.034 | 0.357 | 0.069 | **0.334** | 0.870 | 0.022 |
| $ML_{fp}$OLYP | 0.060 | 0.025 | 0.063 | 0.074 | 1.148 | 0.355 | 1.153 | 2.319 | 0.069 |
| $ML_{1f}$OLYP | 0.066 | 0.023 | 0.084 | 0.057 | 0.729 | 0.129 | 0.580 | 2.153 | 0.048 |
| $ML_{1p}$OLYP | 0.065 | 0.029 | 0.069 | 0.077 | 1.154 | 0.348 | 1.145 | 2.394 | 0.075 |
| $MP_{ff}$OPBE | 0.071 | 0.009 | 0.123 | **0.012** | **0.360** | 0.224 | 0.457 | **0.226** | 0.026 |
| $MP_{fp}$OPBE | 0.039 | 0.012 | 0.045 | 0.044 | 0.478 | 0.057 | 0.436 | 1.255 | 0.019 |
| $MP_{1f}$OPBE | 0.053 | 0.015 | 0.076 | 0.031 | 0.534 | 0.167 | 0.432 | 1.441 | 0.028 |
| $MP_{1p}$OPBE | 0.047 | 0.019 | 0.055 | 0.046 | 0.482 | 0.057 | 0.445 | 1.249 | 0.023 |

[a] results obtained using QZ4P basis set, in **bold** the functional that performs best for that particular property

[b] more information can be found in ref. [21].

# Performance of the Functionals for Structural Characterization of $S_N2$ Stationary Points

Similar to the energetic performance for $S_N2$ reactions, for the structural characterization of their stationary points we also take a look at different components,[21] and compare the DFT results for these with reference values that were obtained with CCSD(T) calculations. Specifically, we look at the bonds and angles for the reactants/products, reactant/product complexes and transition state structures. The mean absolute deviation is then taken for both the bonds and the angles, and the product of these values is then the overall performance $P_G$ for the geometry of $S_N2$ reactions. Previously,[21] we already showed that not only do OPBE and OLYP improve considerably upon PBE for the overall performance for the energy, but also for the geometry. I.e., the $P_G$ value for PBE (0.418) is dramatically reduced for both OPBE (0.042) and OLYP (0.029). Note that the values reported in this chapter are different from the previously reported values,[21] since we take only the data obtained with large basis sets into account here.

The performance of the newly developed functionals for the structural characterization of $S_N2$ reactions is for most cases a clear improvement over the early GGAs, and in many cases also over OLYP/OPBE. In general, the constraint-free functionals (ab=ff) perform significantly better than when constraints are imposed (see table 4). For instance, the $P_G$ value of MP$_{ff}$PBE is small (0.02), while those of the corresponding constrained ones are very large (0.51-0.56), indeed even larger than the already substantial PBE value (0.42). This is however not true for the MP$_{ab}$OPBE functionals that have all $P_G$ values between 0.019 and 0.028. Equally well-performing are MP$_{ff}$OLYP, MP$_{ff}$PBE and several atomic functionals. Extraordinarily good is the A$_{fp}$OPBE functional with a $P_G$ value of only 0.012, i.e. a further reduction by around two compared to OLYP and e.g. the MP$_{ab}$OPBE functionals. This is mainly resulting from the improved description of bonds (for which it has a MAD value of 0.022 Å), and not as much the angles for which the MAD value is similar to that of e.g. OLYP/OPBE. The small MAD value for the distances is, compared to the other functionals, mainly resulting from the RC/PC complexes, for which A$_{fp}$OPBE shows a MAD value of 0.029 Å w.r.t. the CCSD(T) data, which is smaller than that of OPBE and OLYP by a factor of around three. The poorest performance is shown for the A$_{lp}$OLYP functional, with a $P_G$ value of 0.68, which results from the poor performance for both bonds (MAD value 0.15 Å) and angles (MAD value 4.53 deg).

Taking both the $P_E$ and $P_G$ values into consideration, we find that there is no clear relationship between the two in general. Although there are functionals (like ML$_{ff}$OLYP and MP$_{ff}$OPBE) that improve upon OLYP and OPBE for both $P_E$ and $P_G$, there are also many others that do well for one but somewhat less for the other. For instance, the best performing functional for $S_N2$ geometries (A$_{fp}$OPBE) is significantly less accurate for energies. Furthermore, there are many functionals (such as ML$_{fp}$OLYP) that are considerably less accurate for both $S_N2$ energetics and geometries.

# Comparison of PBE with the Simplified PBE (sPBE) and BEE Functionals

So far we have discussed only the (non-constrained) functionals, and how the presence of these affect their performance. However, we would also like to investigate the performance of the sPBE and BEE[84] functionals. As mentioned in the section on the construction of the functionals, the sPBE functional is a simplification of the PBEc correlation functional and uses the original PBEx exchange, while the BEE was determined from a Bayesian Error Estimate[84] and is different from PBE only in the exchange part.

The performance of the sPBE functional is in many cases similar to that of the original PBE functional, both for many of the standard benchmark tests and the $S_N2$ benchmarks. However, there are also some tests where the simplified PBE correlation performs better than the original functional. For instance, the MAD values for the atomization energies of the G2-1 and G2/97 sets are considerably smaller for sPBE (6.8 and 12.9 kcal·mol$^{-1}$) than for PBE (8.0 and 16.3 kcal·mol$^{-1}$), see table 2. Likewise, the MAD value for the hydrogen-bonding distances is also significantly smaller for sPBE (1.9 pm) than for PBE (2.5 pm). Therefore, although for some systems the sPBE functional performs better than PBE, the improvements are not spectacular as was shown by e.g. OPBE for the reaction barriers.

The BEE functional on the other hand is significantly better than either PBE or sPBE for the atomization energies (see table 2), but at the same time significantly worse for the accuracy of geometries of the small molecules and for the weak interactions. For instance, its MAD value for π-π stacking is 10.7 kcal·mol$^{-1}$, and for hydrogen-bonding distances 5.6 pm, which are respectively 3.6 kcal·mol$^{-1}$ and 3.7 pm larger than the sPBE values. For the $S_N2$ benchmarks, it does better than either PBE or sPBE but only marginally so, especially compared to the major improvements shown by OPBE and OLYP.

# Spin-State Splittings of a High-Spin Iron Compound

It was previously shown[45,50] that the OPBE functional works exceptionally well for spin-states of iron complexes, and although we do not have CCSD(T) data to compare with, we know the experimental ground-state of the molecules. Therefore we include here as test on the newly developed functionals the calculation of the spin-state splittings of one of the typical iron compounds, i.e. Fe(N(CH$_2$-o-C$_6$H$_4$S)$_3$)(1-Me-imidazole). Experimentally, and with the OPBE functional, it has a high-spin sextet ground-state with the low-spin doublet and intermediate quartet higher in energy. Similar to what was observed for the energetics of the $S_N2$ reactions, the non-constrained functionals perform better than the constrained ones (see table 5). The majority of the newly developed functionals, however, do not predict the correct spin ground-state. For the ones that do, the largest separation between low- and high-spin is obtained with the MP$_{ff}$OPBE functional (17.3 kcal·mol$^{-1}$), while the A$_{lp}$OPBE predicts all three states at virtually the same energy.

**Table 5. Spin-state splittings (kcal·mol$^{-1}$) for Fe(N(CH$_2$-o-C$_6$H$_4$S)$_3$)(1-Me-imidazole) (see figure 6)**

| functional | doublet | quartet | sextet |
|---|---|---|---|
| PBE | -4.1 | -2.5 | 0 |
| sPBE | -4.4 | -2.7 | 0 |
| BEE | -2.4 | -1.6 | 0 |
| OPBE | 12.4 | 6.3 | 0 |
| OLYP | 7.4 | 4.0 | 0 |
| A$_{ff}$PBE | 2.2 | 0.9 | 0 |
| A$_{fp}$PBE | -2.7 | -1.7 | 0 |
| A$_{1f}$PBE | -4.8 | -2.8 | 0 |
| A$_{1p}$PBE | -4.6 | -2.8 | 0 |
| A$_{ff}$OLYP | 7.3 | 4.0 | 0 |
| A$_{fp}$OLYP | 2.6 | 1.5 | 0 |
| A$_{1f}$OLYP | -16.5 | -9.2 | 0 |
| A$_{1p}$OLYP | -5.0 | -2.6 | 0 |
| A$_{ff}$OPBE | 12.4 | 6.3 | 0 |
| A$_{fp}$OPBE | 7.4 | 3.8 | 0 |
| A$_{1f}$OPBE | -11.9 | -6.9 | 0 |
| A$_{1p}$OPBE | -0.1 | -0.2 | 0 |
| MP$_{ff}$PBE | 5.7 | 3.2 | 0 |
| MP$_{fp}$PBE | -9.7 | -5.2 | 0 |
| MP$_{1f}$PBE | -3.9 | -2.3 | 0 |
| MP$_{1p}$PBE | -9.1 | -4.9 | 0 |
| ML$_{ff}$OLYP | 10.4 | 5.7 | 0 |
| ML$_{fp}$OLYP | -1.3 | -0.6 | 0 |
| ML$_{1f}$OLYP | 1.4 | 0.5 | 0 |
| ML$_{1p}$OLYP | -1.8 | -1.0 | 0 |
| MP$_{ff}$OPBE | 17.3 | 9.2 | 0 |
| MP$_{fp}$OPBE | 2.9 | 1.5 | 0 |
| MP$_{1f}$OPBE | 6.3 | 2.9 | 0 |
| MP$_{1p}$OPBE | 2.8 | 1.2 | 0 |
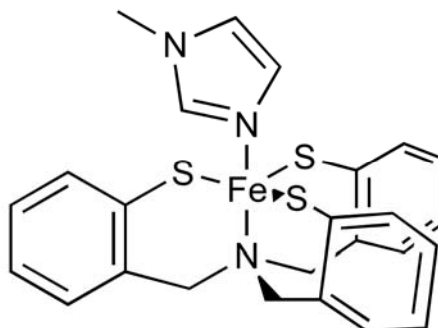


Figure 6. Iron(III) complex Fe(N(CH$_2$-o-C$_6$H$_4$S)$_3$)(1-Me-imidazole).

## Conclusion

We have explored in this chapter what might be the origin of the spectacular improvements of OPBE (and OLYP) over PBE for a number of chemical properties, such as atomization energies, accuracies of geometries and reaction energy profiles. In particular, we have investigated what is the effect of the constraints that are imposed on the PBEx exchange functional, on the one hand by lifting these constraints for the PBEx functional, and on the other by imposing them on the OPTX functional. For all benchmark tests we investigated, the best performance is obtained with one of the newly developed functionals, but unfortunately there is no one that is equally good for all benchmarks.

A comparison of the performance of the $A_{lp}PBE$, $A_{lp}OPBE$ and $A_{lp}OLYP$ shows that the PBEx exchange expression is better suited for the fulfillment of the constraints than is the OPTX expression. The mean absolute deviations are in all these cases lower with the PBEx expression than with the OPTX one. However, these constrained functionals work well only for proton affinities and hydrogen-bonded systems, for the other benchmark tests are the non-constrained functionals working much better. This leads to sometimes extraordinarily good performance, for instance for the accuracy of geometries where the $ML_{ff}OLYP$ functional approaches the accuracy of CCSD(T).

The poor performance for weak interactions by OPBE and related unconstrained functionals does not result from the way how the exchange functional has been obtained. Both the newly developed atomic (e.g. $A_{ff}OPBE$) and molecular (e.g. $MP_{ff}OPBE$) functionals are particularly poor for the weak interactions, which is in some cases improved upon by imposing one (or more) constraint(s). This is especially true for the newly developed functionals based on the PBEx expression that in general do a better job for weak interactions than those based on the OPTX expression. The same is true for the proton affinities, while it is the opposite for the reaction barriers, etc. Therefore, the replacement of $s^2$ as leading term in the PBEx expression by $s^4$ in the OPTX expression is not beneficial for all systems.

### Acknowledgment

## References

[1]    Koch, W.; Holthausen, M. C. *A Chemist's Guide to Density Functional Theory*, Wiley-VCH, Weinheim, 2000.

[2]    Parr, R. G.; Yang, W. *Density functional theory of atoms and molecules*, Oxford University Press, New York, 1989.

[3]    Dreizler, R.; Gross, E. *Density Functional Theory*, Plenum Press, New York, 1995.

[4]    Hohenberg, P.; Kohn, W. *Phys. Rev.* 1964, 136, B864-B871.

[5]   Vosko, S. H.; Wilk, L.; Nusair, M. *Can. J. Phys.* 1980, 58, 1200-1211.

[6]   Perdew, J. P.; Zunger, A. *Phys. Rev. B* 1981, 23, 5048-5079.

[7]   Perdew, J. P.; Wang, Y. *Phys. Rev. B* 1992, 45, 13244-13249.

[8]   Perdew, J. P.; Yue, W. *Phys. Rev. B* 1986, 33, 8800-8802.

[9]   Perdew, J. P.; Tao, J. M.; Staroverov, V. N.; Scuseria, G. E. *J. Chem. Phys.* 2004, 120, 6898-6911.

[10]  Perdew, J. P., in P. Ziesche, H. Eschrig (Eds.), *Electronic structure of Solids* 1991. Akademie, Berlin, 1991, p. 11.

[11]  Becke, A. D. *J. Chem. Phys.* 1993, 98, 5648-5652.

[12]  Perdew, J. P.; Ruzsinszky, A.; Tao, J. M.; Staroverov, V. N.; Scuseria, G. E.; Csonka, G. I. *J. Chem. Phys.* 2005, 123, 062201.

[13]  Fonseca Guerra, C.; Visser, O.; Snijders, J. G.; Velde, G. T.; Baerends, E. J., in E. Clementi, G. Corongiu (Eds.), *Methods and Techniques for Computational Chemistry*, METECC-5. STEF, Cagliari, 1995, p. 303-395.

[14]  Fonseca Guerra, C.; Snijders, J. G.; Velde, G. T.; Baerends, E. J. *Theor. Chem. Acc.* 1998, 99, 391-403.

[15]  Gauss, J.; Stanton, J. F. *Phys. Chem. Chem. Phys.* 2000, 2, 2047-2060.

[16]  Inaba, T.; Sato, F. *J. Comput. Chem.* 2007, 28, 984-995.

[17]  Pollack, L.; Windus, T. L.; De Jong, W. A.; Dixon, D. A. *J. Phys. Chem. A* 2005, 109, 6934-6938.

[18]  Helgaker, T.; Gauss, J.; Jørgensen, P.; Olsen, J. *J. Chem. Phys.* 1997, 106, 6430-6440.

[19]  Bak, K. L.; Jørgensen, P.; Olsen, J.; Helgaker, T.; Klopper, W. *J. Chem. Phys.* 2000, 112, 9229-9242.

[20]  Bak, K. L.; Gauss, J.; Jørgensen, P.; Olsen, J.; Helgaker, T.; Stanton, J. F. *J. Chem. Phys.* 2001, 114, 6548-6556.

[21]  Swart, M.; Solà, M.; Bickelhaupt, F. M. *J. Comput. Chem.* 2007, 28, 1551-1560.

[22]  Bento, A. P.; Solà, M.; Bickelhaupt, F. M. *J. Comput. Chem.* 2005, 26, 1497-1504.

[23]  Swart, M.; Ehlers, A. W.; Lammertsma, K. *Molec. Phys.* 2004, 102, 2467-2474.

[24]  Bento, A. P.; Solà, M.; Bickelhaupt, F. M. *J. Chem. Theor. Comp.* 2008, 4, 929-940.

[25]  Perdew, J. P. *Phys. Rev. B* 1986, 33, 8822-8824. Erratum: Ibid. 8834, 7406.

[26]  Perdew, J. P.; Chevary, J. A.; Vosko, S. H.; Jackson, K. A.; Pederson, M. R.; Singh, D. J.; Fiolhais, C. *Phys. Rev. B* 1992, 46, 6671 Ibid E 6648 (1993) 4978.

[27]  Perdew, J. P.; Burke, K.; Ernzerhof, M. *Phys. Rev. Lett.* 1996, 77, 3865-3868.

[28]  Perdew, J. P.; Burke, K.; Wang, Y. *Phys. Rev. B* 1996, 54, 16533-16539.

[29]  Perdew, J. P.; Kurth, S.; Zupan, A.; Blaha, P. *Phys. Rev. Lett.* 1999, 82, 2544-2547.

[30]  Tao, J. M.; Perdew, J. P.; Staroverov, V. N.; Scuseria, G. E. *Phys. Rev. Lett.* 2003, 91, 146401.

[31]  Staroverov, V. N.; Scuseria, G. E.; Tao, J. M.; Perdew, J. P. *J. Chem. Phys.* 2003, 119, 12129-12137.

[32]  Perdew, J. P.; Burke, K.; Ernzerhof, M. *Phys. Rev. Lett.* 1996, 77, 3865-3868 Erratum 3878 1396.

[33]  Perdew, J. P.; Ernzerhof, M.; Burke, K. *J. Chem. Phys.* 1996, 105, 9982-9985.

[34]  Stephens, P. J.; Devlin, F. J.; Chabalowski, C. F.; Frisch, M. J. *J. Phys. Chem.* 1994, 45, 11623-11627.

[35]  Zhang, Y.; Yang, W. *Phys. Rev. Lett.* 1998, 80, 890.

[36]  Swart, M.; Snijders, J. G. *Theor. Chem. Acc.* 2003, 110, 34-41, Erratum: ibid 111, 156.

[37] Hammer, B.; Hansen, L. B.; Norskov, J. K. *Phys. Rev. B* 1999, 59, 7413.

[38] Adamo, C.; Barone, V. *J. Chem. Phys.* 2002, 116, 5933-5940.

[39] Xu, X.; Goddard III, W. A. *J. Chem. Phys.* 2004, 121, 4068-4082.

[40] Handy, N. C.; Cohen, A. J. *Molec. Phys.* 2001, 99, 403-412.

[41] Becke, A. D. *Phys. Rev. A* 1988, 38, 3098.

[42] Lee, C.; Yang, W.; Parr, R. G. *Phys. Rev. B* 1988, 37, 785.

[43] Cohen, A. J.; Handy, N. C. *Chem. Phys. Lett.* 2000, 316, 160-166.

[44] Baker, J.; Pulay, P. *J. Chem. Phys.* 2002, 117, 1441-1449.

[45] Swart, M.; Groenhof, A. R.; Ehlers, A. W.; Lammertsma, K. *J. Phys. Chem. A* 2004, 108, 5479-5483.

[46] Becke, A. D. *J. Chem. Phys.* 2000, 112, 4020-4026.

[47] Staroverov, V. N.; Scuseria, G. E.; Tao, J.; Perdew, J. P. *J. Chem. Phys.* 2003, 119, 12129-12137.

[48] Van Voorhis, T.; Scuseria, G. *J. Chem. Phys.* 1998, 109, 400-410.

[49] Swart, M.; Ehlers, A. W.; Lammertsma, K. *in preparation* 2009.

[50] Swart, M. *J. Chem. Theory Comput.* 2008, 4, 2057-2066.

[51] Pierloot, K.; Vancoillie, S. *J. Chem. Phys.* 2006, 125, 124303.

[52] Swart, M. *Inorg. Chim. Acta* 2007, 360, 179-189.

[53] Reiher, M.; Salomon, O.; Hess, B. A. *Theor. Chem. Acc.* 2001, 107, 48-55.

[54] Reiher, M. *Inorg. Chem.* 2002, 41, 6928-6935.

[55] Zhao, Y.; Truhlar, D. G. *Theor. Chem. Acc.* 2008, 120, 215-241.

[56] Conradie, J.; Ghosh, A. *J. Chem. Theor. Comp.* 2007, 3, 689-702.

[57] Zhang, Y.-Q.; Luo, C.-L. *J. Phys. Chem. A* 2006, 110, 5096-5101.

[58] Zhang, Y.; Wu, A.; Xu, X.; Yan, Y. *Chem. Phys. Lett.* 2006, 421, 383-388.

[59] Wu, A.; Zhang, Y.; Xu, X.; Yan, Y. *J. Comput. Chem.* 2007, 28, 2431-2442.

[60] Wasbotten, I.; Ghosh, A. *Inorg. Chem.* 2006, 45, 4910-4913.

[61] Groenhof, A. R.; Ehlers, A. W.; Lammertsma, K. *J. Am. Chem. Soc.* 2007, 129, 6204-6209.

[62] Derat, E.; Kumar, D.; Neumann, R.; Shaik, S. *Inorg. Chem.* 2006, 45, 8655-8663.

[63] Romo, S.; Fernández, J. A.; Maestre, J. M.; Keita, B.; Nadjo, L.; De Graaf, C.; Poblet, J. M. *Inorg. Chem.* 2007, 46, 4022-4027.

[64] Rong, C.; Lian, S.; Yin, D.; Shen, B.; Zhong, A.; Bartolotti, L.; Liu, S. *J. Chem. Phys.* 2006, 125, 174102.

[65] Liao, M.-S.; Watts, J. D.; Huang, M.-J. *J. Comput. Chem.* 2006, 27, 1577-1592.

[66] Liao, M.-S.; Watts, J. D.; Huang, M.-J. *J. Phys. Chem. A* 2007, 111, 5927-5935.

[67] Zein, S.; Borshch, S. A.; Fleurat-Lessard, P.; Casida, M. E.; Chermette, H. *J. Chem. Phys.* 2007, 126, 014105.

[68] Conradie, J.; Ghosh, A. *J. Phys. Chem. B* 2007, 111, 12621-12624.

[69] Swart, M.; Güell, M.; Luis, J. M.; Solà, M. *Proceedings of "European Biological Inorganic Chemistry Conference - EUROBIC9"* 2008, 77-82.

[70] Güell, M.; Luis, J. M.; Solà, M.; Swart, M. *J. Phys. Chem. A* 2008, 112, 6384-6391.

[71] Proynov, E. I.; Sirois, S.; Salahub, D. R. *Int. J. Quant. Chem.* 1997, 64, 427.

[72] Grüning, M.: Density functional theory with improved gradient and orbital dependent functionals, PhD thesis, Vrije Universiteit Amsterdam, Amsterdam, 2003.

[73] Zhao, Y.; Truhlar, D. G. *J. Phys. Chem. A* 2008, 112, 6794-6799.

[74] Swart, M.; Van der Wijst, T.; Fonseca Guerra, C.; Bickelhaupt, F. M. *J. Mol. Model.* 2007, 13, 1245-1257.

[75] Van der Wijst, T.; Fonseca Guerra, C.; Swart, M.; Bickelhaupt, F. M. *Chem. Phys. Lett.* 2006, 426, 415-421.

[76] Swart, M.; Bickelhaupt, F. M. *J. Chem. Theor. Comp.* 2006, 2, 281-287.

[77] Swart, M.; Rösler, E.; Bickelhaupt, F. M. *J. Comput. Chem.* 2006, 27, 1486-1493.

[78] Grimme, S. *J. Comput. Chem.* 2004, 25, 1463-1473.

[79] Xu, X.; Goddard III, W. A. *Proc. Natl. Acad. Sci. USA* 2004, 101, 2673-2677.

[80] Cerny, J.; Hobza, P. *Phys. Chem. Chem. Phys.* 2005, 7, 1624-1626.

[81] Keal, T. W.; Tozer, D. J. *J. Chem. Phys.* 2003, 119, 3015-3024.

[82] Waller, M. P.; Robertazzi, A.; Platts, J. A.; Hibbs, D. E.; Williams, P. A. *J. Comput. Chem.* 2006, 27, 491-504.

[83] Swart, M.; Bickelhaupt, F. M. *J. Comput. Chem.* 2008, *29*, 724-734.

[84] Mortensen, J. J.; Kaasbjerg, K.; Frederiksen, S. L.; Nørskov, J. K.; Sethna, J. P.; Jacobsen, K. W. *Phys. Rev. Lett.* 2005, 95, 216401.

[85] Curtiss, L. A.; Raghavachari, K.; Trucks, G. W.; Pople, J. A. *J. Chem. Phys.* 1991, 94, 7221-7230.

[86] Curtiss, L. A.; Raghavachari, K.; Redfern, P. C.; Pople, J. A. *J. Chem. Phys.* 1997, 106, 1063-1079.

[87] Swart, M.; Rösler, E.; Bickelhaupt, F. M. *Eur. J. Inorg. Chem.* 2007, 3646-3654.

[88] Jurecka, P.; Sponer, J.; Hobza, P. *J. Phys. Chem. B* 2004, 108, 5466-5471.

[89] Jurecka, P.; Sponer, J.; Cerny, J.; Hobza, P. *Phys. Chem. Chem. Phys.* 2006, 8, 1985-1993.

[90] Baerends, E. J.; Autschbach, J.; Bérces, A.; Bo, C.; Boerrigter, P. M.; Cavallo, L.; Chong, D. P.; Deng, L.; Dickson, R. M.; Ellis, D. E.; Fan, L.; Fischer, T. H.; Fonseca Guerra, C.; Van Gisbergen, S. J. A.; Groeneveld, J. A.; Gritsenko, O. V.; Grüning, M.; Harris, F. E.; Van Den Hoek, P.; Jacobsen, H.; Van Kessel, G.; Kootstra, F.; Van Lenthe, E.; Mccormack, D. A.; Osinga, V. P.; Patchkovskii, S.; Philipsen, P. H. T.; Post, D.; Pye, C. C.; Ravenek, W.; Ros, P.; Schipper, P. R. T.; Schreckenbach, G.; Snijders, J. G.; Solà, M.; Swart, M.; Swerhone, D.; Te Velde, G.; Vernooijs, P.; Versluis, L.; Visser, O.; Van Wezenbeek, E.; Wiesenekker, G.; Wolff, S. K.; Woo, T. K.; Ziegler, T., ADF 2005.01. SCM, Amsterdam, 2005.

[91] Te Velde, G.; Bickelhaupt, F. M.; Baerends, E. J.; Fonseca Guerra, C.; Van Gisbergen, S. J. A.; Snijders, J. G.; Ziegler, T. *J. Comput. Chem.* 2001, 22, 931-967.

[92] Van Lenthe, E.; Baerends, E. J. *J. Comput. Chem.* 2003, 24, 1142-1156.

[93] Hamprecht, F. A.; Cohen, A. J.; Tozer, D. J.; Handy, N. C. *J. Chem. Phys.* 1998, 109, 6264-6271.

[94] Becke, A. D. *J. Chem. Phys.* 1997, 107, 8554-8560.